Changing chromatin fiber conformation by nucleosome repositioning

Oliver Müller[1], Nick Kepper[2], Robert Schöpflin[1], Ramona Ettig[2], Karsten Rippe[2] and Gero Wedemann[1*]

[1] CC Bioinformatics, University of Applied Sciences Stralsund, Zur Schwedenschanze 15, 18435 Stralsund, Germany

[2] Deutsches Krebsforschungszentrum & BioQuant, 69120, Heidelberg, Germany

[*]Corresponding author

Supporting Material

Supporting Materials and Methods

For a full description of the model and the simulation procedure please see Supplementary Material of ref. (17) and ref. (46), respectively. The description given here follows the presentations in the mentioned work. Generally, chromatin is modeled as a chain of segments, in which nucleosome segments are connected by DNA segments. Each segment has a position and a local coordinate system consisting of three perpendicular unit vectors $(\vec{f}_i, \vec{u}_i, \vec{v}_i)$ that describe the orientation of the ith segment. Vector $\vec{u}_i$ indicates thereby the direction of the segment.

Elastic energies

Elastic interactions are modeled by harmonic potentials. The strength constants of the interactions are named $a_{(Y)}^{(X)}$ where X denotes the type of interaction (s=stretching, b=bending,

t=torsion) and Y the interaction partners (DNA or nucleosome). The energy for stretching is calculated by

$$E_{stretch} = \frac{a_Y^{(s)}}{b_i^0}\left(b_i - b_i^0\right)^2, \quad \text{(S1)}$$

where b_i is the current length and b_i^0 is the equilibrium length of the segment. The bending energy is given by

$$E_{bending} = \frac{a_Y^{(b)}}{b_i^0}{\theta_i}^2, \quad \text{(S2)}$$

where θ_i is calculated from $cos(\theta_i) = \vec{B}_i\vec{u}_{i+1}$ with $\vec{B}_i$ being the equilibrium direction of the next segment and $\vec{u}_{i+1}$ its actual direction. The torsional energy is computed as

$$E_{torsion} = \frac{a_Y^{(t)}}{b_i^0}(\alpha_i + \gamma_i - \tau_i)^2, \quad \text{(S3)}$$

where angles α_i,and γ_i are from the Euler-transformation of $\vec{u}_i$ to $\vec{u}_{i+1}$ with the angles (α_i, β_i, γ_i). The angle α_i describes the rotation around $\vec{u}_i$ and τ_i is the intrinsic twist (87).

Electrostatic energy of linker DNA

Our previous approach for calculating electrostatic interactions of DNA approximated DNA as composed of homogeneously charged cylindrical segments and was restricted to a constant length of linker DNA segments (40). To allow DNA linkers of variable lengths within a simulated chromatin fiber we modeled the DNA linker here by a chain comprised of an arbitrary number of charged spheres as described in the following. The GROMACS unit system was used according to Supplementary Table S1, which is based on *nm*, *ps*, *K*, electron charge (*e*) and atomic mass unit (*u*) (81).

The electrostatic energy of two spheres with charge q_1 and q_2 and radius *a* separated by a center-to-center-distance *r* can be approximated by the electrostatic part of the Derjaguin-Landau-Verwey-Overbeek, DLVO, theory (82, 83) as

$$E_{el}(r) = \frac{1}{4\pi\varepsilon\varepsilon_0} q_1 q_2 \left(\frac{e^{\kappa a}}{1+\kappa a}\right)^2 \frac{e^{-\kappa r}}{r}, \quad \text{(S4)}$$

with κ being the inverse Debye length calculated by:

$$\kappa^2 = \frac{2e_c^2 \rho N_A}{\varepsilon\varepsilon_0 k_B T} . \quad \text{(S5)}$$

For the values listed in Table S1 κ yields $\kappa = 1.0387\, nm^{-1}$ which corresponds to a Debye length of $\lambda_D = \kappa^{-1} = 0.96\, nm$.

The charge of a DNA segment is given by $q = \nu d$, with ν being the nominal line charge density (−2/0.34 e_c nm^{-1}) and *d* the length of the DNA represented by the sphere. The line charge density ν of the DNA must be adapted to the effective charge density ν^*

$$\nu^* = \nu \chi_{CR} \chi_{PBS} , \quad \text{(S6)}$$

where χ_{CR} is the charge adaptation factor and χ_{PBS} accounts for the geometry of subsequent overlapping beads and for deviations due to using an approximation instead of the exact Poisson-Boltzmann (PB) equation (84). Here, we use for χ_{CR} a value of 0.42 as proposed in (84). The adaptation factor χ_{PBS} was determined by relating the new potential to the previous description as cylindrical segments, which was tested in great detail using measurements from single DNA molecule experiments as a benchmark (84). The electrostatic energies computed with equation (S4) for a chain of 100 DNA segments that interact with a single DNA segment were fitted to the values obtained from the PB corrected Debye-Hückel (DH) equation for charged cylinders using finite elements method (84) (data provided by Ralf Seidel). The electrostatic energies as function of distance are plotted for different salt concentrations in Fig. S3. The approximation reproduces the energy curves of the numerical solution very well for the given adaptation factors.

We are aware that our approach using the DLVO-equation for the electrostatic repulsion between two charged spheres could be enhanced by applying the improved Derjaguin approximation (85) as reviewed recently (86). However, this approximation is computationally more demanding. Since the new approximation used here reproduces the previous approximation well, which was tested in great detail (84), it is sufficiently accurate for the numerical simulations of nucleosome chain folding conducted here .

Internucleosomal interaction

The model of the internucleosomal interaction is based on a shifted 12-6 Lennard -Jones potential

$$E_{internuc} = 4\varepsilon(\hat{o}_1, \hat{o}_2, \hat{r}) \left[\left(\frac{\sigma_0}{|\vec{r}| - \sigma(\hat{o}_1, \hat{o}_2, \hat{r}) + \sigma_0} \right)^{12} - \left(\frac{\sigma_0}{|\vec{r}| - \sigma(\hat{o}_1, \hat{o}_2, \hat{r}) + \sigma_0} \right)^{6} \right], \quad \text{(S7)}$$

where $\hat{o}_1$ and $\hat{o}_2$ denote the orientation of the nucleosomes and $\vec{r}$ the distance between the centers of the nucleosomes. The dependency of ε and σ from $\hat{o}_1$, $\hat{o}_2$ and $\hat{r}$ reflects the shape of the nucleosome and is modeled by a series expansion in S-functions (53):

$$\sigma(\hat{o}_1, \hat{o}_2, \hat{r}) = \sigma_0[\sigma_{000} S_{000} + \sigma_{cc2}(S_{202} + S_{022}) + \sigma_{220} S_{220} + \sigma_{222} S_{222} + \sigma_{224} S_{224}], \quad \text{(S8)}$$

and

$$\varepsilon(\hat{o}_1, \hat{o}_2, \hat{r}) = \varepsilon[\varepsilon_{000} S_{000} + \varepsilon_{cc2}(S_{202} + S_{022}) + \varepsilon_{220} S_{220} + \varepsilon_{222} S_{222} + \varepsilon_{224} S_{224}] \quad \text{(S9)}$$

The expansion coefficients were chosen in order to fit the dimensions of a nucleosome and to achieve a ratio of interaction energies of 1/12 between side-by-side and top-on-top oriented nucleosomes. Further details on the energy terms are given in ref. (46) and in the supplemental material of ref. (17). The influence of the nucleosome tails is included in the choice of the strength of ε (46). In principle more details could be added by modifications of the expansion coefficients ε_{xxx}. We refrained from doing so since details of the internucleosomsal interaction are still subject of research and unambiguous experimental evidence for a detailed theoretical model is lacking.

DNA-Nucleosome excluded volume

The volume of DNA segments is approximated by spheres. The minimal distance *d* between the center of a DNA sphere and a spherocylinder describing the nucleosome is computed. The excluded volume $E_{DNA\text{-}Nuc}$ is described as the sum of the individual excluded volume energies $E'_{DNA\text{-}Nuc}$ computed for a DNA sphere and the volume of the nucleosome

$$E'_{DNA-Nuc} = \begin{cases} 0 & if\ d \geq r_n + r_d \\ k(d - r_n - r_d)^{12} & else \end{cases} \quad \text{(S10)}$$

with r_n=(5.5/2) nm and r_d = 1.2 nm.

Simulation protocol

We used a Monte Carlo (MC) algorithm to create a statistical relevant set of configurations satisfying the Boltzmann distribution (54). In order to avoid trapping in local energy minima observed in this kind of systems (46) we applied a replica exchange procedure introduced by Swendsen and Wang (55). Here, *M* replicas of the system were simulated with classical Metropolis Monte Carlo simultaneously, each at a certain temperature T_i, where the single temperatures represent a temperature gradient. After a defined number of MC simulation steps systems with adjacent temperatures (T_i, T_{i+1}) attempted to exchange their replicas with the probability:

$$\min[1, \exp(-(\beta_i - \beta_{i+1})(E_{i+1} - E_i))] \quad \text{(S11)}$$

with $\beta_i = 1/(k_B T_i)$, k_B being the Boltzmann constant and E_i the energy of the system *i*. Thus, a replica is heated and cooled down, respectively, during these exchange events avoiding the systems to get trapped in a local minimum. The temperatures were determined by using a feedback-optimized approach prior to the production run of the simulations (47). This algorithm optimizes the distribution of temperatures at a given maximum temperature iteratively, such that the diffusion of replicas from the highest to the lowest temperature and vice versa is improved in each iteration. The procedure can be made more efficient by starting with a system, that was pre-relaxed utilizing a simulated annealing scheme (46).

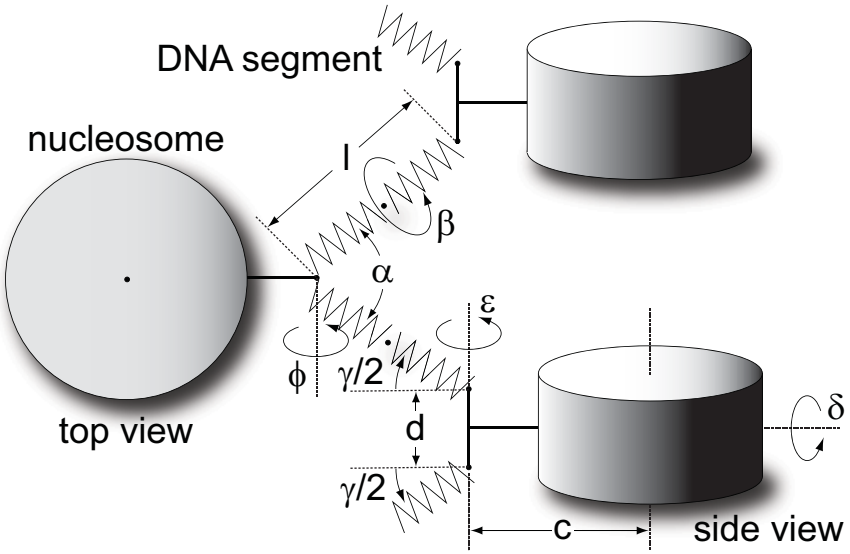

Figure S1: Schematic representation of the elements of the chromatin model (modified from ref. (26)). The angles α, δ, ε, γ describe the orientation of the DNA segments relative to the nucleosome segment, they are connected to. β controls the orientation of the nucleosomes to each other. *l* stands for the length of the DNA modeling the linker DNA, *d* for the distance between the entry and the exit point of the linker DNA at the nucleosome, *c* for the distance between the entry and exit points and the center of the oblate spherocylinder modeling the nucleosome.

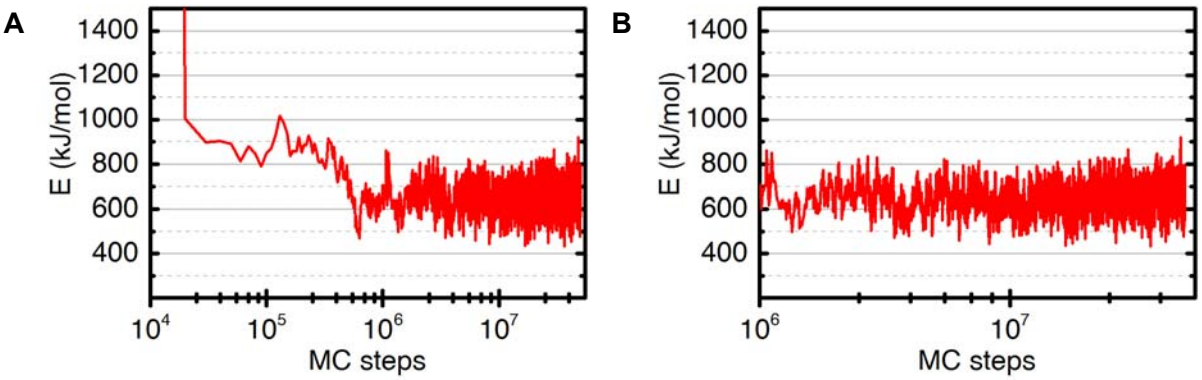

Figure S2: Development of the energy of the replica of the lowest temperature in the simulation of CLS-fiber. (A) All simulation steps. (B) Detailed view for steps larger than 10^6. These data illustrate, that the simulations have reached equilibrium.

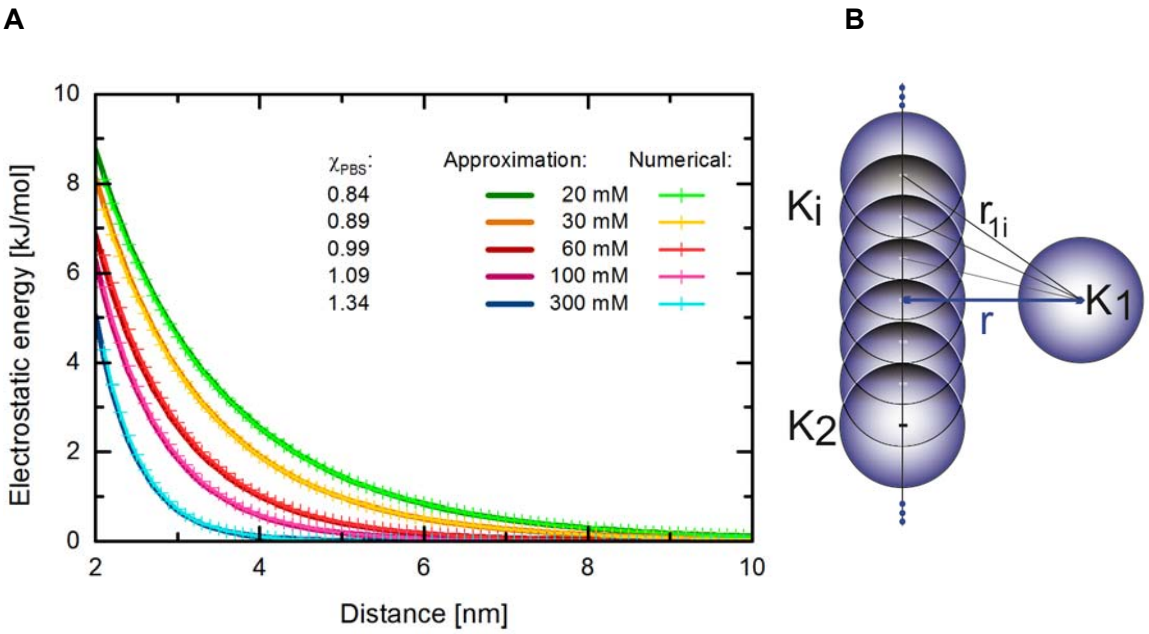

Figure S3. (A) Energies for a chain of 100 DNA segments with a segment length of *d* = 1 nm as a function of the distance *r* to a single segment. Calculations from the more exact method of finite elements (symbols and lighter colors) (84) are shown in comparison to the approximated solution with spherical DNA segments (solid dark lines). For each salt condition the factor χ_{PBS} obtained from the best fit is shown. The sphere radius was set to *a*=1.2 *nm* for all salt conditions. (B) Schematic of the model system used to calculate the electrostatic energies. A single DNA segment K_1 interacts with a chain of DNA segments K_i.

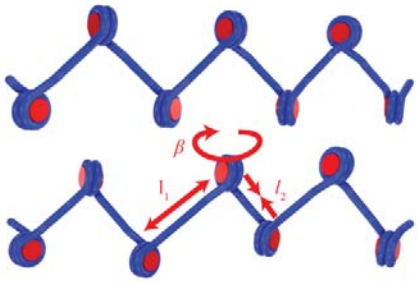

Figure S4. Approach to model nucleosome repositioning. Linker l_1 is lengthened while linker l_2 is simultaneously shortened by the same amount so as to move the center nucleosome towards its right-side neighbor (arrows). The torsional angle β is modified according to the length changes (rotation arrow). Histones are in red, DNA in blue. Higher-order chromatin structure was mostly omitted to facilitate interpretation.

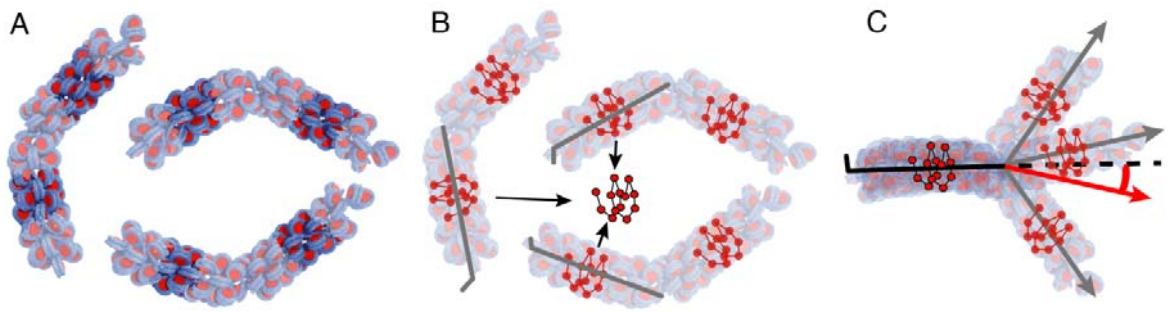

Figure S5. Mean bending angle calculation. (A) Fiber segments representing the middle third of each fiber part are chosen (opaque fiber sections). (B) The chosen segment coordinates of the starting fiber parts (red circles) are used to calculate consensus coordinates (black circles) from all fibers configurations. Grey lines represent the centroid vectors of the respective segment coordinates with the small grey line denoting the rotational position. (C) Fibers are aligned to the consensus coordinates. The rotational positions of the aligned fiber parts now are in agreement with the rotational position of the consensus coordinates (black line). The centroid vectors of the unaligned parts (grey arrows) are calculated from the respective segment coordinates (red circles). The mean bending angle is computed as the angle between the centroid vector of the first part (black) and the vector mean of the centroid vectors of the second part (red arrow).

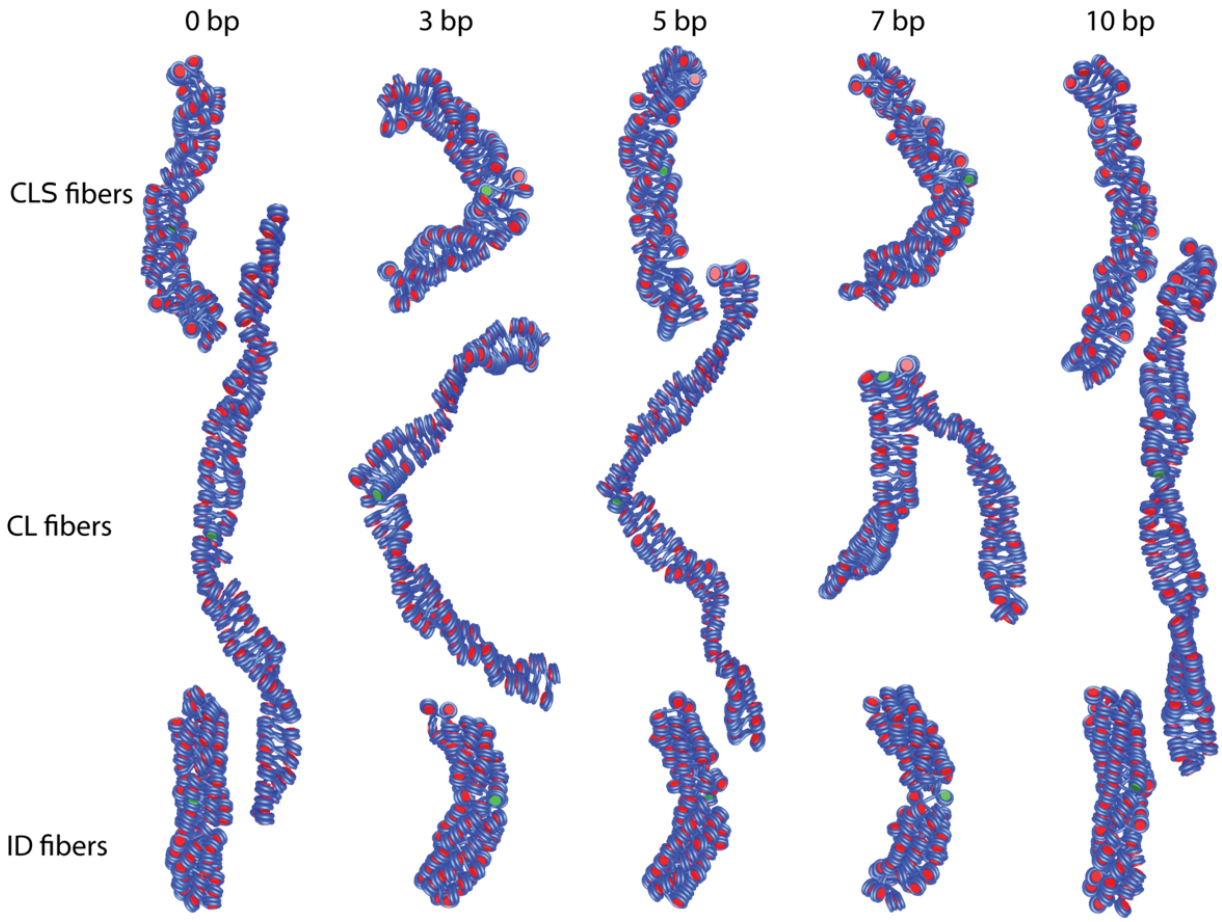

Figure S6. Simulation snapshots of representative conformations from simulated fibers obtained after repositioning the central nucleosome. Fiber type is denoted on the left, repositioning distance at the top. The repositioned nucleosome is shown in green, other nucleosomes in red and DNA in blue. While conformations with d = 5 and d = 10 bp are shaped rather straight, similar to the unmodified conformation, conformations with d = 3 and d = 7 bp appear kinked in the region around the repositioned nucleosome.

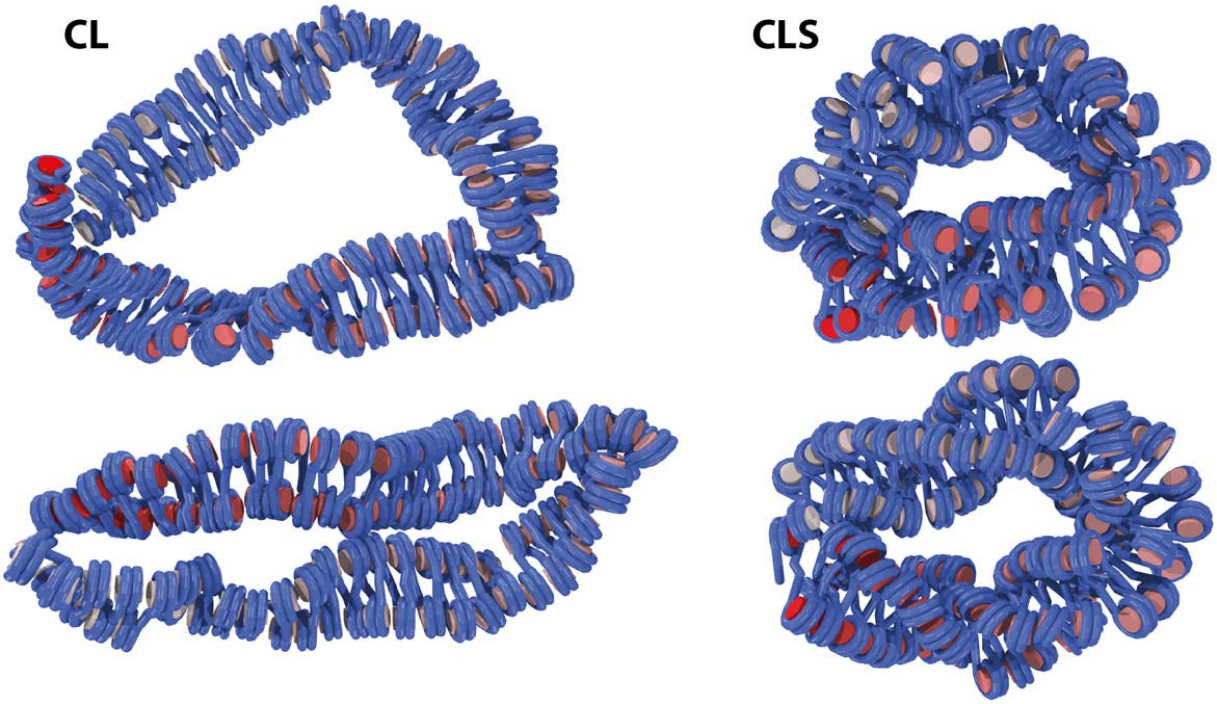

Figure S7. Snapshots of strongly kinked fibers in which the central nucleosome is repositioned by 3 bp. On the left two snapshots of a CL fiber and on the right two snapshots of a CLS fiber are shown. The nucleosomes are colored by their position in the chain (first is white, last is red) and the DNA segments are colored blue.

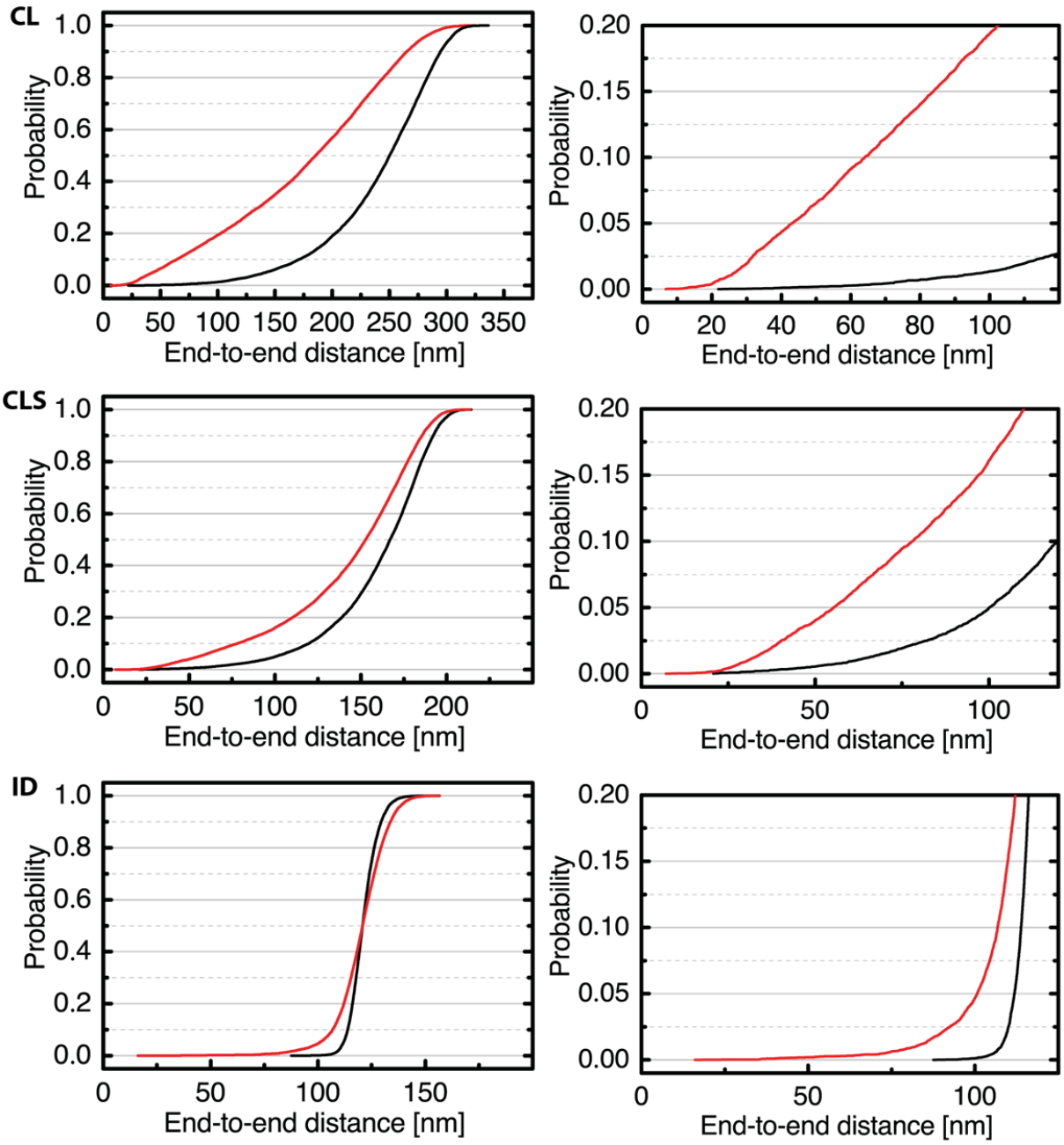

Figure S8. Cumulated probability of the end-to-end distance for the three fiber types shown for unmodified fibers (black curves) and fibers, in which the central nucleosome is displaced by 3 bp (red curves). The plots on the right hand-side show a detailed view of the first 100 nm. The probability of small distances is greatly increased for CL and CLS fibers.

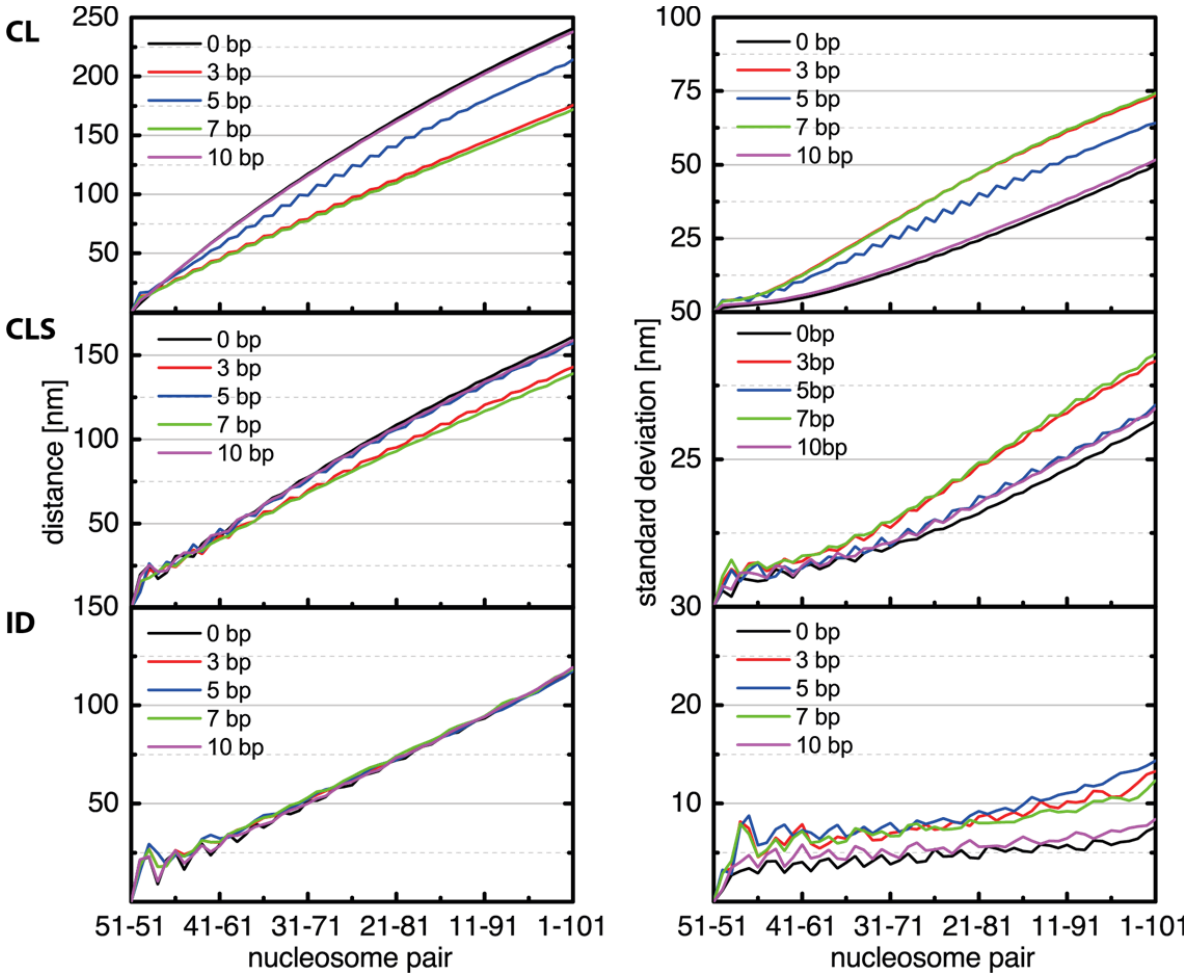

Figure S9. Geometric distance as a function of the genomic distance. For all three fiber models in the left panel the geometric distance is plotted against the genomic distance given by the nucleosome pairs. In the right panel the standard deviation of the geometric distance is plotted.

e_c	**$1.602 \cdot 10^{-19}$ C**	**electric charge unit**
v	$-2/0.34\ e_c\ nm^{-1}$	line charge density of DNA
ρ	$0.1 \cdot 10^{-24}$ mol nm^{-3}	molarity of the monovalent solution
N_A	$6.022 \cdot 10^{23}\ mol^{-1}$	Avogadro constant
ε	80	value for the dielectric value in the solution
ε_0	$(4\pi f)^{-1}$	dielectric constant
f	138.935 kJ nm $mol^{-1}\ e_c^{-2}$	electric conversion factor
k_B	$8.314513 \cdot 10^{-3}$ kJ $mol^{-1}\ K^{-1}$	Boltzmann constant (same as gas constant R)
a	1.2 nm	radius of the DNA model sphere
T	293 *K*	temperature of the solution

Supplementary Table S1: Constants and parameters

Fiber model type	α (°)	β (°)	γ (°)
CLS	26.000	–100.000	0.000
CL	17.713	175.000	–17.713
ID	117.500	355.000	–70.890

Table S2: Structural parameters for the fiber models considered in this work. For a detailed explanation of the chromatin structure model used and the meaning of the respective parameters see Fig. S1 and refer to (17, 40, 46).

Parameter	Value
Temperature	293 K
Ionic strength	100 mM NaCl
Stretching module (DNA)	1.10×10^{-18} J nm
Bending module (DNA)	2.06×10^{-19} J nm
Torsion module (DNA)	2.67×10^{-19} J nm
Electrostatic radius (DNA)	1.2 nm
Stretching module (nucleosome)	1.10×10^{-18} J nm
Torsion module (nucleosome)	1.30×10^{-18} J nm
Interaction potential parameters (nucleosome)	S000 = 1.6957
	Scc2 = –0.7641
	S220 = –0.1480
	S222 = –0.2582
	S224 = 0.5112
	E000 = 2.7206
	Ecc2 = 6.0995
	E220 = 3.3826
	E222 = 7.1036
	E224 = 3.2870
	S000 = 1.6957

Table S3: Parameters used in the Monte Carlo simulations. For a detailed explanation of the stretching, bending and torsion module parameters, refer to (40). An in-depth description of the nucleosomal interaction potential can be found in (17).

Supporting References

1. Stehr, R., R. Schöpflin, R. Ettig, N. Kepper, K. Rippe, and G. Wedemann. 2010. Exploring the conformational space of chromatin fibers and their stability by numerical dynamic phase diagrams. Biophys. J. 98: 1028–1037.

2. Stehr, R., N. Kepper, K. Rippe, and G. Wedemann. 2008. The effect of internucleosomal interaction on folding of the chromatin fiber. Biophys. J. 95: 3677–3691.

3. Klenin, K., H. Merlitz, and J. Langowski. 1998. A Brownian Dynamics Program for the Simulation of Linear and Circular DNA and Other Wormlike Chain Polyelectrolytes. Biophys. J. 74: 780–788.

4. Wedemann, G., and J. Langowski. 2002. Computer simulation of the 30-nanometer chromatin fiber. Biophys. J. 82: 2847–2859.

5. Hess, B., C. Kutzner, D. van der Spoel, and E. Lindahl. 2008. GROMACS 4: Algorithms for Highly Efficient, Load-Balanced, and Scalable Molecular Simulation. J. Chem. Theory Comput. 4: 435–447.

6. Walker, D.A., B. Kowalczyk, M.O. de la Cruz, and B.A. Grzybowski. 2011. Electrostatics at the nanoscale. Nanoscale. 3: 1316–1344.

7. Levin, Y. 2002. Electrostatic correlations: from plasma to biology. Rep. Prog. Phys. 65: 1577.

8. Maffeo, C., R. Schöpflin, H. Brutzer, R. Stehr, A. Aksimentiev, G. Wedemann, and R. Seidel. 2010. DNA-DNA Interactions in Tight Supercoils Are Described by a Small Effective Charge Density. Phys. Rev. Lett. 105: 158101.

9. Sader, J.E., S.L. Carnie, and D.Y.C. Chan. 1995. Accurate Analytic Formulas for the Double-Layer Interaction between Spheres. J. Colloid Interface Sci. 171: 46–54.

10. Nguyen, A.V., L.T.T. Tran, and J.D. Miller. 2012. Particle–Particle Interaction. In: Lee S, KHH Henthorn, editors. Particle technology and applications. Boca Raton, FL: CRC Press. pp. 31–50.

11. Zewdie, H. 1998. Computer simulation studies of liquid crystals: A new Corner potential for cylindrically symmetric particles. J. Chem. Phys. 108: 2117.

12. Metropolis, N., A.W. Rosenbluth, M.N. Rosenbluth, A.H. Teller, and E. Teller. 1953. Equation of State Calculations by Fast Computing Machines. J. Chem. Phys. 21: 1087–1092.

13. Swendsen, and Wang. 1986. Replica Monte Carlo simulation of spin glasses. Phys. Rev. Lett. 57: 2607–2609.

14. Katzgraber, H., S. Trebst, D. Huse, and M. Troyer. 2006. Feedback-optimized parallel tempering Monte Carlo. J Stat Mech Theor Exp. P03018:03018.

15. Rippe, K., R. Stehr, and G. Wedemann. 2012. Monte Carlo Simulations of Nucleosome Chains to Identify Factors that Control DNA Compaction and Access. In: Schlick T, editor. Innovations in Biomolecular Modeling and Simulations. Cambridge: Royal Society of Chemistry. pp. 198–235.